

Lines of Evidence for Horizontal Gene Transfer of a Phenazine Producing Operon into Multiple Bacterial Species

David A. Fitzpatrick

Received: 19 August 2008 / Accepted: 12 January 2009 / Published online: 3 February 2009
© Springer Science+Business Media, LLC 2009

Abstract Phenazines are secondary metabolites with broad-spectrum antibiotic activity against bacteria, fungi, and eukaryotes. In pseudomonad species, a conserved seven-gene phenazine operon (*phz*ABCDEFGF) is required for the conversion of chorismic acid to the broad-spectrum antibiotic phenazine-1-carboxylate. Previous analyses of genes involved in phenazine production from nonpseudomonad species uncovered a high degree of sequence similarity to pseudomonad homologues. The analyses undertaken in this study wished to elucidate the evolutionary history of genes involved in the production of phenazines. Furthermore, I wanted to determine if the phenazine operon has been transferred through horizontal gene transfer. Analyses of GC content, codon usage patterns, frequency of 3:1 dinucleotides, sequence similarities, and phylogenetic reconstructions were undertaken to map the evolutionary history of phenazine genes from multiple bacterial species. Patchy phyletic distribution, high sequence similarities, and phylogenetic evidence infer that pseudomonad, *Streptomyces cinnamonensis*, *Pantoea agglomerans*, *Burkholderia cepacia*, *Pectobacterium atrosepticum*, *Brevibacterium linens*, and *Mycobacterium abscessus* species all contain a phenazine operon which has most likely been transferred among these species through horizontal gene transfer. The acquisition of an antibiotic-

associated operon is significant, as it may increase the relative fitness of the recipient species.

Keywords Horizontal gene transfer · Phenazines · Phenazine operon · GC content · Phylogenetic analysis · 3:1 dinucleotide frequency

Introduction

Horizontal gene transfer (HGT) can be defined as the non-vertical transmission of genes between different strains or species. HGT between different bacterial species can act as an evolutionary factor driving genetic diversity (Jain et al. 2003; Ochman et al. 2000). Gene transfer can alter the biochemical properties of a recipient organism and has the potential to create functional novelties allowing for the exploitation of unfamiliar environments (Ochman et al. 2000). HGT has been associated with the gain of genes that confer the ability to catabolize certain amino acids that are important virulence factors (Martin et al. 1998) and, also, the acquisition of drug resistance by benign bacteria (Woo et al. 2003). Large-scale genomic sequencing of prokaryotes has revealed that gene transfer is an important evolutionary mechanism for these organisms (Eisen 2000; Jain et al. 2003). It has been suggested that HGT is so rampant, that the prokaryote tree of life is more net-like than tree-like (Doolittle 1999). However, there is much debate as to whether lateral gene transfer is an ubiquitous influence throughout prokaryotic genome evolution. Some authors suggest that alternative explanations such as gene loss, gene duplication, and the segregation of paralogues are incorrectly described as HGT events (Kurland et al. 2003).

This analysis investigated the evolutionary history of an operon normally associated with the production of

Electronic supplementary material The online version of this article (doi:10.1007/s00239-009-9198-5) contains supplementary material, which is available to authorized users.

D. A. Fitzpatrick (✉)
Department of Biology, National University of Ireland,
Maynooth, Co. Kildare, Ireland
e-mail: david.fitzpatrick@nuim.ie

secondary metabolites (phenazines) in pseudomonad species. Phenazines are biologically active, water-soluble chorismic acid derivatives (Giddens et al. 2002; Mavrodi et al. 1998). They are produced by diverse eubacteria, including members of the *Streptomyces*, *Pseudomonas*, *Pelagiobacter*, *Vibrio*, *Erwinia*, and *Burkholderia* genera (Imamura et al. 1997; Sato et al. 1995; Turner and Messenger 1986), and are often excreted at high levels during bacterial growth in vitro (Mavrodi et al. 2006). Phenazines have a characteristic tricyclic ring system and have been shown to confer a selective growth advantage to organisms which secrete them, as they possess broad-spectrum antibiotic activity toward bacteria, fungi, and eukaryotes (Blankenfeldt et al. 2004). Phenazine antibiotic activity is linked to their ability to undergo oxidation-reduction transformations leading to the accumulation of toxic superoxide radicals in target cells (Hassett et al. 1993).

In pseudomonad species, the best-studied phenazine producers, a conserved seven-gene phenazine (phz) operon (*phz*ABCDEFG) is required for the conversion of chorismic acid to the broad-spectrum antibiotic phenazine-1-carboxylate (PCA) (Mavrodi et al. 1998, 2001; Parsons et al. 2004b). Genes belonging to this operon are referred to as core phenazine genes in this analysis. In *P. aeruginosa* PAO1, the *phz* operon is present in duplicate, each copy possessing the ability to produce PCA (Mavrodi et al. 2001). Initial Southern hybridization studies showed that the *phz* operon was present in 21 phenazine producing pseudomonads, but not in 7 phenazine producing isolates of *Burkholderia* and *Brevibacterium* (Mavrodi et al. 2001). This led to the supposition that the *phz* operon is conserved in pseudomonads and may be unique to them (Mavrodi et al. 2001). However, subsequent analyses have located *phz*-like operons in phenazine producing species such as *Streptomyces cinnamomensis*, *Pantoea agglomerans*, *Burkholderia cepacia*, and *Pectobacterium atrosepticum* species (Bell et al. 2004; Giddens et al. 2002; Haagen et al. 2006; Mavrodi et al. 2006).

This analysis set out to elucidate the evolutionary history of *phz* operons from a diverse range of bacteria. I also wished to determine if there is evidence that any of the sequenced bacteria in GenBank contain the *phz* operon.

The overall patchy phyletic distribution, aberrant phylogenies, evidence of gene linkage, and high sequence similarities provide evidence that multiple components of a core phenazine biosynthesis operon found in pseudomonad, *Streptomyces cinnamomensis*, *Pantoea agglomerans*, *Burkholderia cepacia*, *Pectobacterium atrosepticum*, *Brevibacterium linens*, and *Mycobacterium abscessus* species shares a similar evolutionary history. Furthermore, it is possible that the *phz* operon disseminated from one of these species to the others via HGT.

Materials and Methods

Sequence Data and Database Searches

Amino acid sequences from all completely sequenced prokaryotic genomes were obtained from the NCBI ftp site (release 165). The genomes utilized and their taxonomic affiliations are listed in Supplemental Table 1. Complete bacterial genomes were utilized so as to ensure potential phenazine operons could be located. Draft protein-coding genes for *Brevibacterium linens* BL2 were downloaded from the DOE Joint Genome Institute. Phenazine gene clusters for *Pseudomonas aeruginosa* PAO1 (AF005404), *Pantoea agglomerans* Eh1087 (AF451953), and *Streptomyces cinnamomensis* (AM384985) were obtained from GenBank. All sequence data were merged to produce a local database.

Seven phenazine genes (*phz*ABCDEFG) from a *Pseudomonas aeruginosa* PAO1 *phz* operon were used as database query sequences. Taking one *phz* protein at a time, gene families were located using the BlastP algorithm (Altschul et al. 1997) with a cutoff expectation (E) value of 10^{-20} .

Accession numbers for all sequences used in this analysis are given by Supplemental Table 2.

Phylogenetic Methods

Gene families were aligned using MUSCLE (v3.6) (Edgar 2004), with the default settings.

Obvious alignment ambiguities were manually corrected. Phylogenetic relationships were inferred for full and representative datasets using maximum likelihood methods. Appropriate protein models of substitution were selected for each gene family using ModelGenerator (Keane et al. 2006). Optimum models and associated parameters for all protein families are summarized in Supplemental Table 3.

One hundred bootstrap replicates were then carried out with the appropriate protein model using the software program PHYML (Guindon and Gascuel 2003) and summarized using the majority-rule consensus method.

Bayesian and LogDet phylogenies based on reduced datasets were also reconstructed for selected gene families (*phz*A/B and *phz*E). Bayesian phylogenies were reconstructed with the software PhyloBayes version 2.3, which incorporates the heterogeneous CAT site model (Lartillot and Philippe 2004). Markov chains were run for 40,000 cycles, discarding the first 10,000 points and then saving a point every 5 cycles. The “bpcomp” command from PhyloBayes was used to ensure that Bayesian trees had converged. A neighbor-joining tree based on amino acid LogDet distances (Lockhart et al. 1994) was

reconstructed using LDDIST (Tholleson 2004), the fraction of invariant sites was estimated by the method of Sidow et al. (1992), and these were excluded. Support for groups on trees were determined using the bootstrap resampling technique.

The approximately unbiased test of phylogenetic tree selection (Shimodaira 2002) was performed, to assess whether differences in topology between constrained and unconstrained gene trees are no greater than expected by chance.

Dinucleotide Frequencies

The distribution of 3:1 dinucleotide frequencies in the whole genomes of *Burkholderia cepacia* R18194, *Pectobacterium atrosepticum* SCRI1043, *Mycobacterium abscessus*, *Brevibacterium linens* BL2, and a representative pseudomonad (*P. aeruginosa* PA01) were determined with CODONW (<http://codonw.sourceforge.net>). The Spearman rank correlation coefficient (Snedecor and Cochran 1995) was used to assess the pairwise covariation of the 3:1 dinucleotide frequencies.

Codon Usage

To determine if *phz* genes had a different codon usage pattern to their host genome, an analysis of variation in synonymous codon usage was undertaken using the GCUA software (McInerney 1998). Individual correspondence analyses of raw codon counts for the genomes of *B. cepacia*, *P. atrosepticum*, *B. linens*, *M. abscessus*, and a representative pseudomonad (*P. aeruginosa* PA01) were performed, with the first four principal axes being used to evaluate synonymous codon usage patterns. Similar analyses were also carried out on the *phz* gene families displayed in Supplemental Figs. 3–7.

Results

Blast Analysis

Using the seven genes (*phzA–G*) from a *Pseudomonas aeruginosa* PA01 *phz* operon as database query sequences, *phz* gene families were located in the bacterial database used in this analysis. Examination of result files showed that many species contain various *phz* homologues. The complete genomes of *B. cepacia*, *P. atrosepticum*, *B. linens*, and *M. abscessus* were found to contain at least four of the seven *phz* genes (Table 1). Furthermore, these genes were localized to specific chromosomal regions, suggesting that they may form operons. A second round of database

searches showed that the *phz* genes within these organisms share relatively high sequence similarity to pseudomonad species (Table 1). Phenazine operons have previously been characterized in *P. agglomerans* and *S. cinnamomensis* (Giddens et al. 2002; Haagen et al. 2006). Phenazine genes from these also share a high sequence similarity to pseudomonad species (Table 1).

Therefore, an initial Blast analysis suggests that core *phz* genes in Pseudomonad, *S. cinnamomensis*, *P. agglomerans*, *B. cepacia*, *P. atrosepticum*, *B. linens*, and *M. abscessus* species are homologous and, due to their relatively high sequence similarity (Table 1), may share a common evolutionary history.

Chromosomal Organization of Phenazine Genes

The chromosomal locations of *phz* genes from *S. cinnamomensis*, *P. agglomerans*, *B. cepacia*, *P. atrosepticum*, *B. linens*, and *M. abscessus* were determined and their organization was compared to that of a characterized *P. aeruginosa* *phz* operon (Mavrodi et al. 2001).

S. cinnamomensis contains six of the seven-core phenazine biosynthesis genes found in *P. aeruginosa*. A *phzF* homologue is absent in *S. cinnamomensis*. Ignoring this and the position of one of the *phzA/B* homologues, the order of the remaining *phz* genes is identical to that in *P. aeruginosa* (Fig. 1).

P. agglomerans contains 16 genes required for the production of a phenazine compound (D-alanylgriseoluteic acid) (Giddens et al. 2002). Homologues for five of the core pseudomonad phenazine producing genes are present within this cluster. *P. agglomerans* does not contain a homologue of *phzC* and has a single copy of *phzA/B*. The organization of the remaining *phz* genes is analogous to that observed in *P. aeruginosa* (Fig. 1).

B. cepacia contains six of the seven *phz* genes found in *P. aeruginosa*. It is missing one of the *phzA/B* homologues (Fig. 1). Overall the organization of the *phz* homologues in *B. cepacia* resembles that of *P. aeruginosa* (Fig. 1). The notable exception is the chromosomal position of *phzC*, which is separated from the remaining phenazine genes by two open reading frames (Fig. 1).

P. atrosepticum contains five core phenazine biosynthesis genes. It contains one *phzA/B* copy and is missing *phzC*. The organization of the phenazine genes also resembles that of *P. aeruginosa* (Fig. 1). There is a predicted open reading frame (ECA2700) separating *phzE* and *phzF*. However, this is most probably a false gene call, as it is short (116 amino acids) and has no significant database hits in GenBank.

B. linens contains seven phenazine homologues. Two copies of *phzD* were located. Three of the phenazine genes (*phzA/B*, *phzD*, and *phzE*) are found in close proximity to

Table 1 List of core phenazine homologues found in six bacterial species; top BlastP database hits and sequence identity are also listed

Species	Gene	BlastP best-hit	Identity
<i>Burkholderia cepacia</i>	phzA/B	<i>Pseudomonas aeruginosa</i> PA7	61%
	phzC	<i>Xanthomonas axonopodis</i>	65%
	phzD	<i>Pseudomonas aeruginosa</i> PA7	61%
	phzE	<i>Pseudomonas aeruginosa</i> PA7	54%
	phzF	<i>Pseudomonas aeruginosa</i> PA14	60%
	phzG	<i>Streptomyces cinnamomensis</i>	50%
<i>Pectobacterium atrosepticum</i>	phzA/B	<i>Streptomyces cinnamomensis</i>	67%
	phzD	<i>Pseudomonas aeruginosa</i> PA7	49%
	phzE	<i>Pseudomonas aeruginosa</i> PA7	44%
	phzF	<i>Pseudomonas aeruginosa</i> PA7	52%
	phzG	<i>Burkholderia cepacia</i>	43%
<i>Pantoea agglomerans</i>	phzA/B	<i>Pseudomonas aeruginosa</i> C3719	59%
	phzD	<i>Salmonella typhimurium</i> LT2	45%
	phzE	<i>Pseudomonas aeruginosa</i> PA7	40%
	phzF	<i>Pseudomonas aeruginosa</i> PA14	45%
	phzG	<i>Pseudomonas aeruginosa</i> PACS2	40%
<i>Brevibacterium linens</i>	phzA/B	<i>Pseudomonas aeruginosa</i> PA7	66%
	phzC	<i>Arthrobacter aurescens</i> TC1	66%
	phzD ₁	<i>Vibrio harveyi</i>	52%
	phzD ₂	<i>Streptomyces cinnamomensis</i>	49%
	phzE	<i>Pseudomonas fluorescens</i>	44%
	phzF	<i>Mycobacterium marinum</i>	61%
	phzG	<i>marine actinobacterium</i>	53%
<i>Mycobacterium abscessus</i>	phzC	<i>Streptomyces cinnamomensis</i>	58%
	phzC	<i>Mycobacterium marinum</i>	87%
	phzD	<i>Pantoea agglomerans</i>	46%
	phzD	<i>Pseudomonas fluorescens</i>	63%
	phzE	<i>Pseudomonas aeruginosa</i> PA7	58%
<i>Streptomyces cinnamomensis</i>	phzG	<i>Paracoccus denitrificans</i>	44%
	phzA/B	<i>Pseudomonas fluorescens</i>	78%
	phzA/B	<i>Pseudomonas fluorescens</i>	52%
	phzC	<i>Pseudomonas aeruginosa</i> PA7	63%
	phzD	<i>Pseudomonas aeruginosa</i> PA7	68%
	phzE	<i>Pseudomonas chlororaphis</i>	61%
	phzG	<i>Pseudomonas fluorescens</i>	55%

one another. However, the organization of this putative phz operon differs to what is observed in *P. aeruginosa* (Fig. 1). The remaining phenazine homologues (*phzC*, *phzF*, *phzG*, and the second copy of *phzD*) are not linked and are dispersed in the *B. linens* genome (not shown).

M. abscessus has six phz biosynthesis homologues. It has two copies of *phzC* and *phzD*. Three of the phenazine homologues (*phzC*, *phzD*, and *phzE*) are linked (Fig. 1). An open reading frame (MAB_0296) splits *phzC* and *phzD*; otherwise their organization is similar to that of *P. aeruginosa* (Fig. 1). The remaining homologues (*phzG* and the second copies of *phzC* and *phzD*) show no evidence of linkage (not shown).

GC Content

The complete genomes of *B. cepacia*, *P. atrosepticum*, *B. linens*, and *M. abscessus* are available. GC content analysis for individual phenazine genes from these species and a representative pseudomonad (*P. aeruginosa* PA01) shows that in general they are in the range observed for the global GC content of their corresponding genome (Table 2). This suggests that if the phenazine biosynthesis genes in these species did originate from an alien source, their GC content has ameliorated (so that it now resembles the host genomes) over time (Lawrence and Ochman 1997). A small number of genes are exceptions, however.

Fig. 1 Comparison of phenazine loci from multiple bacterial species with *P. aeruginosa* PAO1. Gene names are shown within gene boxes. Homologues are also color-coded. *B. linens* and *M. abscessus* have additional homologues (not shown) but they are not linked to the putative phenazine operon

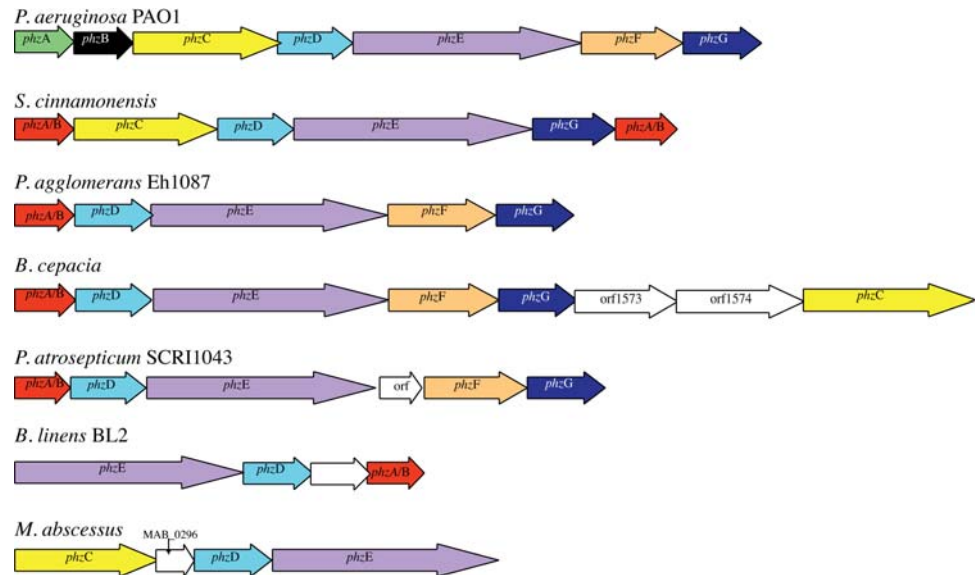


Table 2 GC content of phenazine homologues found in six bacterial species; where applicable, the GC content for each genome is also listed

	<i>phzA/B</i>	<i>phzC</i>	<i>phzD</i>	<i>phzE</i>	<i>phzF</i>	<i>phzG</i>	Average genome GC content
<i>P. aeruginosa</i> PAO1	60.94%	72.49%	70.51%	70.22%	68.04%	71.62%	66%
	52.14%						
<i>B. cepacia</i>	61.41%	63.89%	61.21%	66.25%	63.64%	65.57%	65.1%
<i>P. atrosepticum</i>	38.77%	N/A	42.83%	49.25%	53.07%	52.58%	48.5%
<i>M. abscessus</i>	NA	66.66%	61.84%	62.68%	N/A	66.81%	62.0%
		65.51%	62.26%				
<i>B. linens</i>	57.69%	62.07%	61.09%	58.30%	N/A	65.17%	61.3%
			58.46%				
<i>P. agglomerans</i>	40.04%	NA	42.87%	44.51%	46.52%	47.20%	56%
<i>S. cinnamomensis</i>	63.59%	72.87%	72.43%	72.67%	N/A	71.80%	~70%
	67.64%						

For example, *phzA/B* from *P. atrosepticum* has a GC content ~10% lower than the average of their host genome (Table 2).

The *phz* core operon from *P. agglomerans* exhibits a GC content of 44.6%. *P. agglomerans* is yet to be sequenced, however, its GC is thought to be approximately 56% (Giddens et al. 2002). Such a deviation in GC may be the result of a successful HGT that has not yet ameliorated to their hosts genomes.

The genome of *S. cinnamomensis* has not been sequenced either. A number of *Streptomyces* species have been sequenced and their GC contents were found to be ~70% (Bentley et al. 2002; Ikeda et al. 2003; Ohnishi et al. 2008). Based on this, the GC content of the *S. cinnamomensis* phenazine genes appear to be in the range of other *Streptomyces* genomes (Table 2).

3:1 Dinucleotide Frequencies

The covariation of 3:1 (the third base of a codon followed by the first base of the proceeding codon) dinucleotide frequencies of the *phz* genes in *B. cepacia*, *P. atrosepticum*, *B. linens*, *M. abscessus*, and *P. aeruginosa* PAO1 relative to their corresponding genomes were evaluated using the Spearman rank correlation coefficient (Supplemental Table 4). These nucleotides are subject to the weakest selective constraints, therefore mutational events are tolerated to a greater degree (Rosas-Magallanes et al. 2006). *p*-values < 0.0001 were observed for the majority of phenazine genes in all organisms (Supplemental Table 4). This infers that the 3:1 dinucleotide frequencies of most phenazine genes display strong covariation with their corresponding genome; this does not suggest evidence

of HGT. There are a small number of exceptions, however. *p*-values of 0.921 and 0.1037 indicate that the 3:1 dinucleotide frequencies of *phzA/B* and *phzD* from *P. atrosepticum* do not exhibit covariation with the 3:1 dinucleotide frequencies of the *P. atrosepticum* genome (Supplemental Table 4). Interestingly, these three genes also display a deviant GC content relative to the *P. atrosepticum* genome (Table 2). Similarly, *phzA/B* from *B. linens* displays a *p*-value of 0.1074 for 3:1 dinucleotide frequencies.

Codon Usage

A correspondence analysis of codon usage in the sequenced genomes of *B. cepacia*, *P. atrosepticum*, *B. linens*, and *M. abscessus* and a representative pseudomonad (*P. aeruginosa* PA01) was undertaken (Supplementary Fig. 1). This was performed so the codon usage of *phz* genes could be compared to the global codon usage of their corresponding genomes. Greater distances from the origin correspond to greater differences in codon usage from the mean values. Therefore vertically descended genes such as essential housekeeping genes are expected to cluster around the origin. Conversely recently acquired genes often display an atypical codon preference compared to other genes in the genome and are expected to be found as outliers (Medigue et al. 1991).

The majority of phenazine genes were found to have a codon usage consistent with the rest of their genomes (Supplementary Fig. 1). Two exceptions are the *phzA/B* and *phzD* genes from *P. atrosepticum* (Supplementary Fig. 1). These two genes also show deviant GC (Table 2) and 3:1 dinucleotide frequencies (Supplementary Table 4) relative to their host genome.

Individual analyses of the variation in synonymous codon usage for all *phz* gene families were also undertaken (Supplementary Fig. 2). However, there is no evidence of a shared codon usage pattern for core phenazine genes in pseudomonad, *S. cinnamomensis*, *B. cepacia*, *P. atrosepticum*, *M. abscessus*, or *B. linens* species (Supplementary Fig. 2).

Phylogenetic Analyses

PhzA/B Phylogeny

The PhzA/B amino acid sequence from *P. aeruginosa* PA01 was used as a query to locate bacterial homologues from the database. The exact roles played by PhzA/B in phenazine production are unknown. However, they may help prevent unproductive decomposition of PCA. Furthermore, the overall yield of PCA has been shown to be

dependent on PhzA in a dose-dependent manner (McDonald et al. 2001).

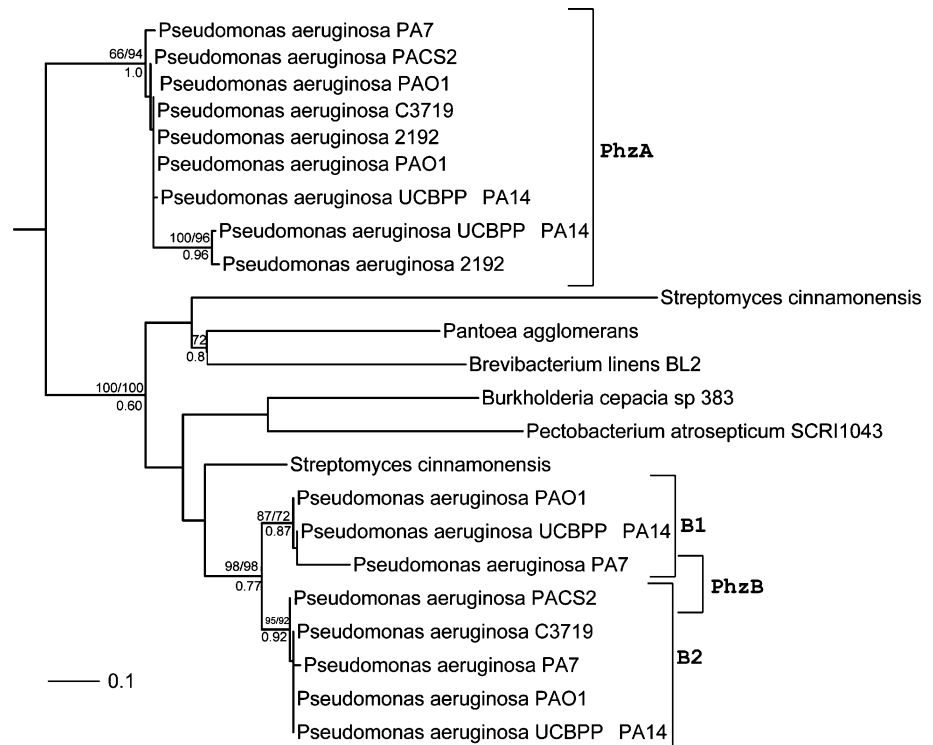
Previous analysis has been shown that pseudomonad *phzB* sequences share a high sequence similarity to *phzA* homologues and are the result of a recent duplication event (Mavrodi et al. 1998). Therefore, *phzB* homologues were also included in this phylogenetic analysis. In total 23 *phzA/B* homologues were located within 11 organisms. Most originated from pseudomonad species. However, homologues were located within the Actinobacteria (*S. cinnamomensis* and *B. linens*), the Enterobacteriales (*P. agglomerans* and *P. atrosepticum*), and the β -proteobacteria (*B. cepacia*). *S. cinnamomensis* was found to contain two PhzA/B proteins. Homologues were not located in any of the remaining 154 γ -proteobacteria species (Supplementary Table 1) or any other bacterial species represented in the database used in this analysis. *P. aeruginosa* PA01 is known to contain two *phz* operons (Mavrodi et al. 2001). Multiple copies of *phzA/B* were also found in *P. aeruginosa* UCBPP-PA14, suggesting that this may also contain two *phz* clusters; all were included for comparative purposes. Maximum likelihood (ML), LogDet, and Bayesian phylogenies were reconstructed from an alignment of all PhzA and PhzB proteins (Fig. 2).

The resultant phylogenies place the *P. agglomerans*, *S. cinnamomensis*, *B. linens*, *B. cepacia*, and *P. atrosepticum* PhzA/B representatives beside the pseudomonad *phzB* homologues with varying degrees of support (Fig. 2; 100% bootstrap support [BP] and 0.60 Bayesian posterior probability [BPP], respectively).

A constrained tree that grouped pseudomonad *phzA* and *phzB* homologues as sister-group taxa, to the exclusion of the nonpseudomonad *phzA/B* homologues, was reconstructed (not shown). A second constrained tree that grouped the nonpseudomonad taxa with pseudomonad *phzA* homologues was also reconstructed. The approximately unbiased test of phylogenetic tree selection (AU test) (Shimodaira 2002) showed that the topologies of the unconstrained (Fig. 2) and the two constrained trees (not shown) are not significantly different. Therefore, one cannot confidently infer that the nonpseudomonad organisms represented in this analysis have gained a pseudomonad *phzB* homologue rather than a *phzA* copy as inferred by the phylogeny (Fig. 2). However, the patchy phylogenetic distribution coupled with the high sequence similarity suggests that the nonpseudomonad organisms represented in Fig. 2 may have gained a pseudomonad copy of *phzA/B* through HGT.

Both phylogenies infer that there is strong phylogenetic support showing the differentiation between the two *phzB* copies in *P. aeruginosa* PA01 and *P. aeruginosa* UCBPP-PA14 (Fig. 2; 98% BP and 0.77 BPP). Neither, ML, LogDet, nor Bayesian phylogenies could differentiate between the two *phzA* genes found in these organisms, however.

Fig. 2 PhzA/B maximum likelihood/LogDet/Bayesian phylogeny. Maximum likelihood and LogDet bootstrap scores are displayed above branches. Bayesian posterior probabilities are shown below selected branches. Pseudomonad PhzA and PhzB homologues are found in separate clades. Nonpseudomonad homologues are branched beside PhzA proteins. According to the AU test this inference is not robust, however



PhzC Phylogeny

Using the PhzC amino acid sequence from *P. aeruginosa* PAO1 as a query sequence, 192 bacterial PhzC homologues from 172 organisms were located. Homologues were confined to the phyla of Actinobacteria and Proteobacteria, except for one Bacteroidetes representative (*Salinibacter ruber* DSM 13855). *B. linens* and *B. cepacia*, *S. cinnamomensis*, and *M. abscessus* all contain a homologue. However, homologues were not located in the closely related plant pathogen *P. atrosepticum* or *P. agglomerans*.

PhzC encodes a 3-deoxy-D-arabino-heptulosonate-7-phosphate (DAHP) synthase and redirects intermediate products from primary metabolism into phenazine biosynthesis (Mavrodi et al. 1998). DAHP synthase is also the first step in the shikimate pathway and catalyzes the condensation of phosphoenolpyruvate and erythrose-4-phosphate (Mavrodi et al. 1998).

A PhzC ML phylogeny for all 192 homologues was reconstructed (Supplemental Fig. 3). For display purposes a second reduced phylogeny was also reconstructed for representative homologues (Fig. 3).

Both *M. abscessus* and *S. cinnamomensis* PhzC proteins are found beside the pseudomonad core PhzC proteins in a strongly supported clade (Fig. 3 and Supplemental Fig. 3; clade A, 100% BP). This inference is consistent with the Blast analysis (Table 1). Pseudomonad species contain multiple DAHP synthase homologues. For example, as well as containing the two *phzC* genes found in core

phz operons, *P. aeruginosa* PAO1 and UCBPP-PA14 have a third DAHP family member, which groups with other pseudomonad homologues (Supplemental Fig. 3; clade B, 100% BP). This *Pseudomonas*-specific clade is found within a large proteobacterial clade (Supplemental Fig. 3). Interestingly, the clade (clade A) that contains the pseudomonad core PhzC proteins shares a sister-group relationship with an Actinomycetales-specific clade (Fig. 3 and Supplemental Fig. 3; 90% and 61% BP) to the exclusion of the large proteobacterial-specific clade (Supplemental Fig. 3). The most parsimonious explanation for this inference is that the last common ancestor of the *Pseudomonas* species represented in this analysis gained a *phzC* gene from an Actinomycetales source that has been subsequently retained after multiple *Pseudomonas* speciation events. Interestingly, *M. abscessus* has a second *phzC* gene but it is grouped with homologues from other mycobacterial species (Supplemental Fig. 3); this is also consistent with the Blast analysis (Table 1). A constrained phylogeny that places the *M. abscessus* homologue found in clade A (Supplemental Fig. 3), with the other Mycobacterial species was reconstructed (not shown). The AU test of phylogenetic tree selection, showed that the original unconstrained tree (groups *M. abscessus* with pseudomonad core PhzC) receives the optimal likelihood tree score, and the difference in likelihood score compared to the constrained tree is significant ($p < 0.00001$).

Overall there are three likely scenarios to explain this inference.

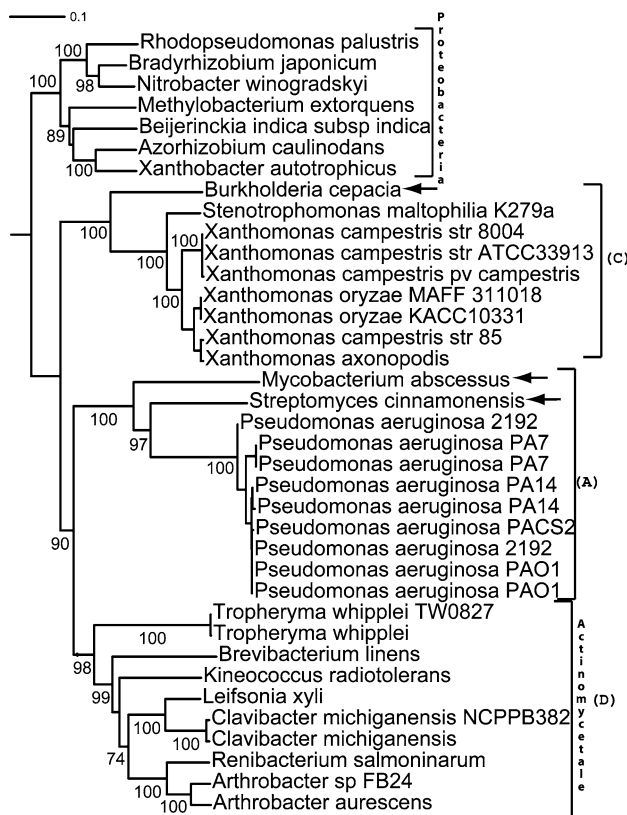


Fig. 3 PhzC maximum likelihood phylogeny. Bootstrap scores are displayed above selected branches. The pseudomonad core PhzC homologues are found in clade A. *B. cepacia* located in clade C with a number of xanthomonad species. *B. linens* is clustered with other Actinobacteria in clade D. All nonpseudomonad core Phz proteins are highlighted with arrows

1. *M. abscessus* may have obtained the core PhzC protein via HGT from *S. cinnamomensis* or an unsampled Actinomycetales bacterium.
2. The *M. abscessus* core PhzC may be the result of a gene duplication followed by a phase of accelerated evolution. The *M. abscessus* core PhzC gene may have then been transferred to *S. cinnamomensis* and a pseudomonad ancestral species.
3. Finally, a pseudomonad ancestral species may have originally gained an Actinomycetales copy of *phzC* from clade D (Fig. 3 and Supplementary Fig. 3) through HGT. This Actinomycetales/*Pseudomonas* homologue may have consequently been transferred to *M. abscessus* and *S. cinnamomensis* via interphyla gene transfer.

The *B. cepacia* *phzC* homologue is grouped beside xanthomonad species (Fig. 3 and Supplemental Fig. 3; clade C, 100% BP). This finding is consistent with the Blast analysis that showed *Xanthomonas axonopodis* to be *B. cepacia*'s top database hit (Table 1). This *Burkholderial* xanthomonad clade does not share a sister-group

relationship with either the large proteobacterial- or Actinomycetales-specific clades (Supplemental Fig. 3). Of the 19 complete *Burkholderia* genomes included in this analysis, only *B. cepacia* has a *phzC* homologue. Scenarios to explain this phylogenetic inference include the fact that *B. cepacia* may have gained *phzC* from a xanthomonad source. Similarly *phzC* may have originated through gene duplication in *B. cepacia* and spread via HGT to an ancestral xanthomonad species, or vice versa. However, a second xanthomonad species *Stenotrophomonas maltophilia* is found in clade C (Supplemental Fig. 3), therefore a single transfer from a xanthomonad donor into *B. cepacia* is most likely. Interestingly *phzC* in *B. cepacia* is separated from the remaining core *Burkholderia* phenazine genes by two genes (Fig. 1).

The *B. linens* *phzC* homologue is grouped beside other actinobacterial species (Fig. 3 and Supplemental Fig. 3; clade D). This inference is again consistent with the Blast analysis that showed actinobacterial species to be *B. linens*'s top DAHP synthase database hit (Table 1). Based on this phylogeny *B. linens* *phzC* is similar to that found in other Actinomycetales species and does not appear to have undergone interphyla gene transfer.

PhzD Phylogeny

Homologues for 107 PhzD proteins from 92 organisms were located through the database search. Homologues were located in the Firmicutes, Actinobacteria, and Proteobacteria. *S. cinnamomensis*, *P. agglomerans*, *B. cepacia*, *P. atrosepticum*, *B. linens*, and *M. abscessus*, all contain a copy of *phzD*. *B. linens* actually has two homologues. Therefore the *phzD* gene is universal to all putative phenazine operons of interest (Fig. 1).

The *phzD* gene encodes a protein belonging to the isochorismatase enzyme family (Mavrodi et al. 1998). In phenazine biosynthesis PhzD transforms 2-amino-4-deoxychorismic acid to 2,3-dihydro-3-hydroxyanthranilic acid (DHHA). The structure of PhzD is similar to a subfamily of α/β -hydrolase enzymes (Parsons et al. 2003). However, PhzD lacks a nucleophilic cysteine found in its relatives and catalyzes unrelated chemistry (Parsons et al. 2003). All PhzD homologues used in this analysis lack the nucleophilic cysteine. They have the characteristic isochorismatase glycine at the analogous position instead (not shown).

Complete and representative PhzD ML phylogenies were reconstructed (Supplemental Fig. 4 and Fig. 4). The pseudomonad core PhzD proteins are grouped together in a strongly supported clade (Fig. 4 and Supplemental Fig. 4; clade A). A large strongly supported proteobacterial clade is evident and does not include the pseudomonad species (Supplemental Fig. 4; clade B, 88% BP). The *B. cepacia*,

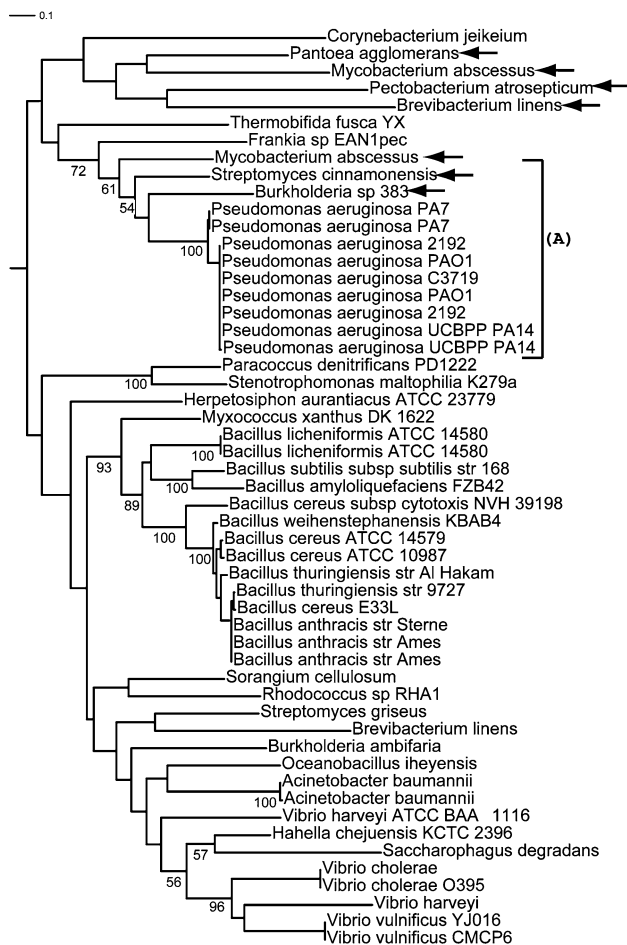


Fig. 4 PhzD maximum likelihood phylogeny. Bootstrap scores are displayed above selected branches. The pseudomonad core PhzD homologues are found in clade A. Nonpseudomonad core PhzD proteins are highlighted with *arrows*. The majority of proteobacterial species represented in this analysis are located in clade B

M. abscessus, and *S. cinnamomensis* isochorismatase enzymes are grouped among the pseudomonad species with moderate support (Fig. 4; 61% BP). The grouping of these three species with the pseudomonad species is unsurprising, as they are >60% identical at the amino acid level (Table 1). Two additional actinobacterial (*Thermobifida fusca* and *Frankia* EAN1pec) species are found at the base of this clade. The most parsimonious explanation for the grouping of these proteins (Fig. 4; clade A) involves gene transfers from an actinobacterial donor into the last common ancestor of all pseudomonads and a second independent transfer into *B. cepacia*. An alternative explanation is that an ancestral pseudomonad species gained an actinobacterial *phzD* homologue, and this has subsequently been transferred back into a number of actinobacterial species; this would have required at least four independent transfers into actinobacterial species, however.

The *B. linens*, *P. agglomerans*, and *P. atrosepticum* PhzD homologues are grouped beside the pseudomonad

representatives, but this inference is poorly supported (Fig. 4 and Supplemental Fig. 4). The weak phylogenetic support for these and other inferences is likely the result of a short PhzD protein (<200 amino acids) with low levels of phylogenetic information. A ML phylogeny was also constructed from a nucleotide equivalent alignment (third positions removed). Similar inferences and support values were also observed (not shown). Therefore based on this phylogeny one cannot confidently elucidate the evolutionary history of the core *phzD* genes in *B. linens*, *P. agglomerans*, and *P. atrosepticum*.

PhzE Phylogeny

Database searches found homologues for 69 PhzE enzymes in 61 species. The majority of homologues were located in the Proteobacteria ($\alpha = 30$, $\gamma = 21$, $\beta = 1$, $\delta = 2$) and Actinobacteria, although members of the Cyanobacteria (*Anabaena* PCC 7120 and *Nostoc punctiforme*) and *Deinococcus-Thermus* (*Deinococcus geothermalis* and *Thermus thermophilus*) phyla are also present. Multiple species have paralogous copies of PhzE (Supplemental Table 2). *S. cinnamomensis*, *P. agglomerans*, *B. cepacia*, *P. atrosepticum*, *B. linens*, and *M. abscessus* all contain a copy of *phzE*. Therefore, as with *phzD*, the *phzE* gene is universal to all putative phenazine operons studied in this analysis (Fig. 1). The PhzE protein is approximately three times larger than PhzD (> 600 amino acids); therefore it should be a more reliable phylogenetic marker.

PhzE is involved in the first step of phenazine biosynthesis. At the sequence level it is similar to anthranilate synthase and converts chorismate, the end product of the shikimate pathway, to 2-amino-4-deoxychorismic acid anthranilate (McDonald et al. 2001).

ML phylogenies based on all 69 PhzE homologues (Supplemental Fig. 5) and selected representatives were reconstructed (Fig. 5). As with other Phz proteins, the pseudomonad core PhzE enzymes are found in a highly supported clade (Fig. 5 and Supplemental Fig. 5; clade A, 100% BP). The *B. cepacia*, *M. abscessus*, and *S. cinnamomensis* homologues form a moderately supported sister-group relationship with the pseudomonad proteins (Fig. 5; 55% BP). These phylogenetic inferences are consistent with the Blast analysis that showed pseudomonad proteins to be *B. cepacia*, *M. abscessus*, and *S. cinnamomensis* top database hits (Table 1). The phylogeny reconstructed using representative homologues places *P. agglomerans*, *B. linens*, and *P. atrosepticum* in a large clade that contains the pseudomonad PhzE homologues (Fig. 5; 99% BP). This inference contradicts the phylogeny based on all 69 PhzE homologues, which places these three species at the base of clade B (Supplemental Fig. 5). The PhzE proteins from *P. agglomerans*, *B. linens*, and *P. atrosepticum* have a high

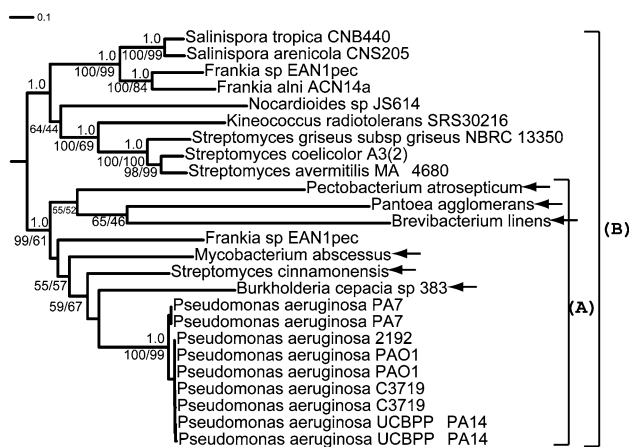


Fig. 5 PhzE maximum likelihood phylogeny. Maximum likelihood and LogDet bootstrap scores are displayed below branches. Bayesian posterior probabilities are shown above selected branches. The pseudomonad core PhzE homologues are found in clade A. Nonpseudomonad core Phz proteins are highlighted with arrows and are also located in clade A. The remaining organisms in clade B are actinobacterial

evolutionary rate illustrated by their long-branch lengths (Fig. 5). Therefore the PhzE phylogeny may be suffering from long-branch attraction artifacts (LBA). To help rule out LBA, Bayesian and LogDet phylogenies based on the reduced dataset were reconstructed (Fig. 5). The Bayesian phylogeny utilized a heterogeneous site model that performs well compared to other methods against phylogenetic artifacts, such as long-branch attraction (Lartillot et al. 2007). The resultant phylogenies infer that the PhzE homologues from *P. agglomerans*, *B. linens*, and *P. atrosepticum* do indeed form a sister-group relationship with the core pseudomonad, *B. cepacia*, *S. cinnamonensis*, and *M. abscessus* PhzE proteins (Fig. 5; clade A, 1.0 BPP and 61% BP).

Interestingly, *P. agglomerans*, *P. atrosepticum*, *B. cepacia*, and *Pseudomonas* are all proteobacteria. The remaining species grouped in clade B are all Actinobacteria (Fig. 5 and Supplemental Fig. 5). All remaining proteobacterial species are grouped together in a separate clade (Supplemental Fig. 5; clade C, 100% BP). A constrained phylogeny with Proteobacteria- and Actinobacteria-specific clades was reconstructed (not shown). The AU test of phylogenetic tree selection showed that the original unconstrained tree (Supplemental Fig. 5) has a significantly better ($p < 0.00001$) likelihood score than the constrained phylogeny. There are a number of possible explanations for this finding. For example, an ancestral Actinobacteria may have gained a proteobacterial PhzE from a close relative of one of the proteobacterial species represented in clade B (Fig. 5). More likely is the suggestion that the core *phzE* gene present in the proteobacterial species (*Pseudomonas*, *B. cepacia*, *P. agglomerans*, and *P. atrosepticum*) in clade B

(Fig. 5 and Supplemental Fig. 5) originated from an Actinomycetale source. However, as with *phzC* and *phzD* an interphyla transfer of *phzE* from an actinobacterial donor into one of the non-Actinobacterial species followed by multiple transfers into the remaining species clustered in clade A (Fig. 5 and Supplemental Fig. 5) is also plausible.

As already mentioned, both *phzD* and *phzE* are universal to all putative phenazine operons of interest (Fig. 1). Furthermore, in relative terms they are congruent with one another with respect to the branching order of all species containing a putative *phz* operon (Figs. 5, 6). However, certain PhzD inferences, in particular, the phylogenetic placement of *P. agglomerans*, *P. atrosepticum*, and *B. linens* beside the other core PhzD proteins is not strongly supported, probably because of the low phylogenetic signal in this protein. Therefore, it would be interesting to determine if there is coevolution between PhzD and PhzE. This hypothesis cannot be tested in an AU framework, however, as both PhzD and PhzE phylogenies have different constituent taxa.

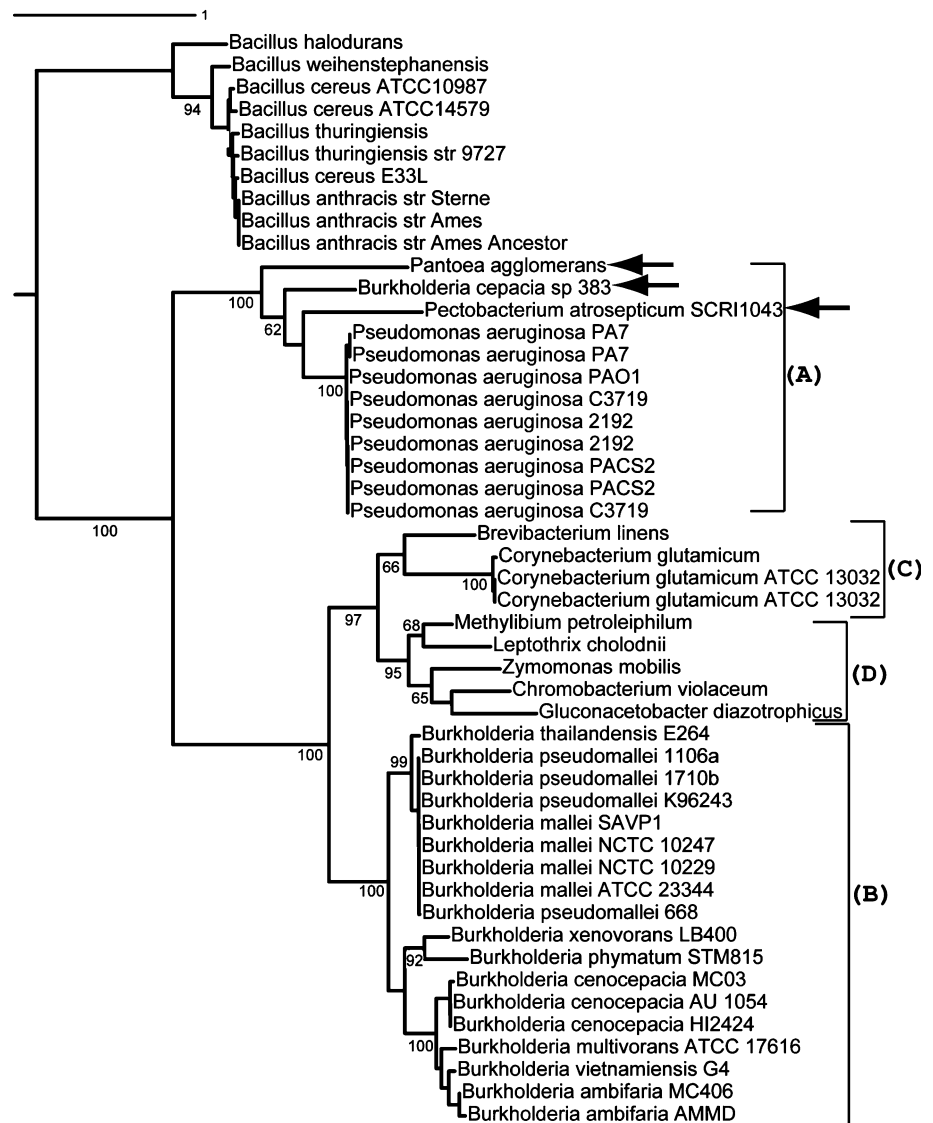
PhzF Phylogeny

A database search located 114 PhzF homologues in 99 prokaryotic organisms. The majority of PhzF homologues are found in Firmicutes and proteobacterial species. However, *phzF* genes were also located in Cyanobacteria, Actinobacteria, and a small number of Archaeal organisms (*Natronomonas pharaonis* and halobacterial species). Homologues were not located in the genomes of *M. abscessus* or *S. cinnamonensis*.

PhzF is a key enzyme in the biosynthesis of phenazines. Biochemical analysis has shown that PhzF is the first step in the dimerization of DHAA to to the broad-spectrum antibiotic PCA (Parsons et al. 2004b). It is similar in structure to the lysine biosynthetic enzyme diaminopimelate epimerase but lacks the same catalytic residues (Blankenfeldt et al. 2004). The PhzF active site has been previously characterized (Blankenfeldt et al. 2004; Parsons et al. 2004b), and all PhzF proteins used in this analysis contain the active center residues.

ML phylogenies for full and representative PhzF homologues were reconstructed. A strongly supported core pseudomonad clade is evident (Fig. 6 and Supplementary Fig. 6; clade A, 100% BP). *B. cepacia*, *P. agglomerans*, and *P. atrosepticum* all form sister-group relationships with the pseudomonad *phzF* homologues (Fig. 6 and Supplemental Fig. 6; clade A, 100% BP). Interestingly homologues from multiple *Burkholderia* species are also present. These are grouped together in a strongly supported clade that does not include the *B. cepacia* PhzF protein (Fig. 6 and Supplemental Fig. 6; clade B). A constrained phylogeny that groups all *Burkholderia* homologues

Fig. 6 PhzF maximum likelihood phylogeny. Bootstrap scores are displayed above selected branches. All nonpseudomonad core Phz proteins are highlighted with arrows. The pseudomonad core PhzF homologues are found in clade A. *B. cepacia*, *P. atrosepticum*, and *P. agglomerans* form a sister-group relationship with the pseudomonad PhzF homologues (clade A). A number of Burkholderia homologues are also present and are located in clade B. *B. linens* is grouped with other actinobacterial species in clade C



together was reconstructed (not shown). The AU test of phylogenetic tree selection inferred that the original unconstrained tree (Fig. 6) has a significantly better likelihood score than the constrained tree ($p < 0.00001$). This is consistent with the hypothesis that *B. cepacia* has gained a PhzF homologue either via HGT or through gene duplication. If it has gained a gene through duplication, this has subsequently been transferred to all other species found in clade A (Fig. 6 and Supplemental Fig. 6). Overall it is not possible to definitely determine the origin of the core *phzF* copies found in clade A, as it does not form a robust sister-group relationship with other clades (Supplemental Fig. 6). However, based on the strongly supported phylogenetic inference, all PhzF proteins found in clade A have a common evolutionary history (Fig. 6 and Supplemental Fig. 6). Multiple scenarios are possible. For example, the core *phzF* gene may have originated de novo in

pseudomonad species and subsequently transferred via HGT to *B. cepacia*, *P. agglomerans*, and *P. atrosepticum*. Conversely the *phzF* gene may have originated in *B. cepacia*, *P. agglomerans*, or *P. atrosepticum* and consequently transferred to all species and the last common ancestor of the pseudomonad species in clade A (Fig. 6 and Supplemental Fig. 6). Another possibility is that all organisms in clade A gained the *phzF* gene from a bacterial genus that is not represented in the genome database yet. Regardless of the direction of the transfer event, it is clear that all core *phzF* genes in clade A (Fig. 6) share a common evolutionary history.

The evolutionary history of the *B. linens* *phzF* homologue is intriguing. It is found in an Actinomycetales-specific clade (Fig. 6 and Supplemental Fig. 6; clade C), which is itself grouped within a large, predominantly proteobacterial clade (Fig. 6 and Supplemental Fig. 6).

Furthermore the Actinomycetales-specific clade is grouped beside a strongly supported α/β -proteobacterial clade (Fig. 6 and Supplemental Fig. 6; clade D). Therefore both PhzE phylogenies (Fig. 6 and Supplemental Fig. 6) led to the conclusion that an ancestral Actinomycetales species most likely gained a PhzE homologue from a proteobacterial source. For completeness a constrained tree that places the *B. linens* PhzF protein beside the core PhzF copies found in clade A (Fig. 6) was reconstructed (not shown). According to the AU test this constrained phylogeny is significantly worse than the original unconstrained tree (Fig. 6). Therefore phylogenetic analysis infers that *B. linens* has not acquired its *phzF* gene from the same donor source as the species found in clade A. Furthermore the *B. linens* *phzF* is located outside the putative phenazine operon (Fig. 1). This leads to the hypothesis that the *phzF* homologue found in *B. linens* is most likely not a core *phzF* homologue and has a different evolutionary history relative to *B. cepacia*, *P. atrosepticum*, *P. agglomerans*, and pseudomonad species *phzF* found in clade A (Fig. 6 and Supplemental Fig. 6).

PhzG Phylogeny

Following database searches, 202 PhzG homologues were located in 192 bacterial species. The majority of PhzG homologues used in this analysis are found in the proteobacterial phylum, although representatives from Actinobacteria, Cyanobacteria, and *Deinococcus* are also present. PhzG homologues were located in *S. cinnamomensis*, *P. agglomerans*, *B. cepacia*, *P. atrosepticum*, and *M. abscessus*. A homologue was not located for *B. linens*.

PhzG is a flavin-dependent oxidase (Parsons et al. 2004a). Even though the three-dimensional crystal structure of PhzG has been solved, the specific reaction catalyzed by PhzG in phenazine biosynthesis is unknown (Parsons et al. 2004a). Structural data have shown that PhzG is very similar to the gene product (pyridoxine-5'-phosphate oxidase) of *Escherichia coli* *pdxH*. It has been proposed that PhzG arose through duplication of *pdxH* (Parsons et al. 2004a).

PhzG phylogenies were reconstructed based on full and representative datasets (Supplementary Fig. 7 and Fig. 7). Pseudomonad core PhzG proteins are clustered together and form a strongly supported sister-group relationship with *M. abscessus*, *S. cinnamomensis*, *P. agglomerans*, *P. atrosepticum*, and *B. cepacia* (Fig. 7 and Supplementary Fig. 7; clade A). This is in agreement with the initial Blast analysis (Table 1).

Further examination of PhzG phylogenies shows that a second pseudomonad clade is evident (Fig. 7 and Supplementary Fig. 7; clade B). Homologues from multiple *Burkholderia* species are also present, including a second

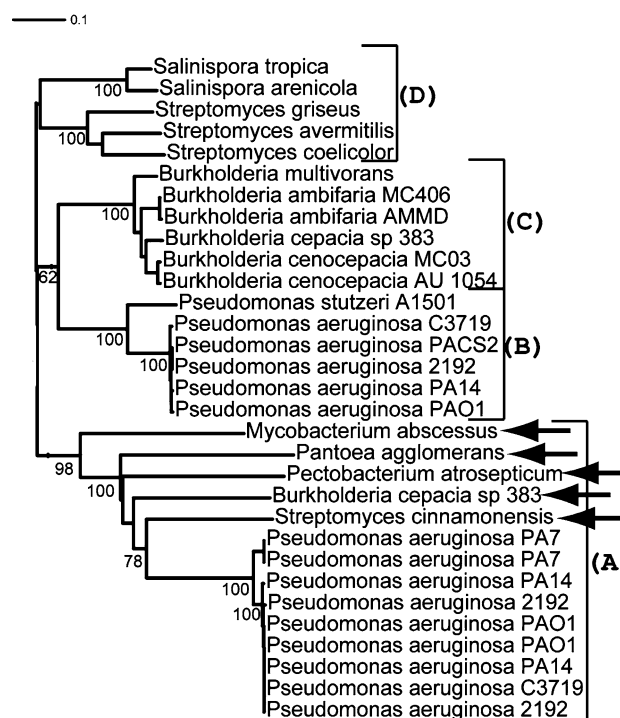


Fig. 7 PhzG maximum likelihood phylogeny. Bootstrap scores are displayed above selected branches. All nonpseudomonad core Phz proteins are highlighted with arrows. The pseudomonad core PhzG homologues are found in clade A. *B. cepacia*, *P. atrosepticum*, *P. agglomerans*, *S. cinnamomensis*, and *M. abscessus* all form a sister-group relationship with the pseudomonad PhzG homologues (clade A). Additional pseudomonad homologues are found in clade B. The majority of *Burkholderia* species represented in this analysis are found in clade C

B. cepacia PhzG homologue (Fig. 7 and Supplementary Fig. 7; clade C). Similarly there is also an actinobacterial-specific clade (Fig. 7 and Supplementary Fig. 7; clade D). Further investigation revealed that all homologues found in clades B, C, and D are actually PdxH proteins. A constrained phylogeny that grouped all *Burkholderia* species together (including the *B. cepacia* homologue found in clade A) was constructed (not shown). Similarly, constrained phylogenies that grouped all pseudomonad proteins and all actinobacterial species together were also constructed (not shown). According to the AU test, the original unconstrained tree receives a significantly better likelihood score than all three constrained trees ($p < 0.00001$). These results show that the core *B. cepacia*, *S. cinnamomensis*, and *M. abscessus* and PhzG proteins in clade A do not match their species phylogeny. As with PhzF, multiple scenarios are possible for these inferences, including a de novo origin of PhzF through gene duplication in any one of the species found in clade A, followed by gene transfer to the remaining species in that clade (Fig. 7 and Supplementary Fig. 7).

Discussion

Phenazines are secondary metabolites with broad-spectrum antibiotic activity. In pseudomonad species, a conserved seven-gene operon is involved in the production of these antibiotics from chorismic acid. Initially it was thought that this seven-gene operon was unique to pseudomonad species, however, further analyses have located *phz*-like operons in a diverse range of phenazine producing bacterial species. Subsequent analyses of *phz* genes in nonpseudomonad species uncovered a high degree of sequence similarity to pseudomonad homologues. This has led to the hypothesis that the *Pseudomonas* *phz* operon may have crossed the species/phylum barrier into other bacterial species via HGT.

In this analysis I wished to elucidate the evolutionary history of the *phz* operon and determine if there is evidence of interphylum gene transfer. Comparative analyses were performed on core phenazine genes and their host genomes to determine if common sequence features of HGT could be detected. In general, GC content (Table 2), codon usage (Supplemental Fig. 1), and 3:1 dinucleotide frequencies (Supplemental Table 4) were consistent between the host genome and the core *phz* genes. A small number of exceptions did exist, however. For example, an analysis of the *P. agglomerans* phenazine operon revealed an atypical GC content relative to its genome (Table 2). Furthermore, 3:1 dinucleotide frequencies and GC contents of *phzA/B* and *phzD* genes of *P. atrosepticum* are divergent from the rest of its genome (Supplemental Table 4). These two anomalies in sequence composition have been shown to be associated with HGT. *P. atrosepticum* and *P. agglomerans* are closely related plant pathogens. If HGT of core *phz* genes has occurred into these species, it was most likely into their last common ancestor. However, the *P. atrosepticum* phenazine operon is embedded within its genome, while the *P. agglomerans* operon is associated with an extra chromosomal plasmid. Operon transfer via plasmids has been observed previously (Rosas-Magallanes et al. 2006). Therefore two independent transfer events cannot be ruled out.

Phylogenetic reconstructions undertaken in this analysis show that the *phz* operon found in pseudomonad and nonpseudomonad species (Fig. 1) shares a common evolutionary history and has most likely moved between species through HGT. For example Figs. 2–7 show that the majority of *phz* genes located in the *phz* operon (Fig. 1) share sister-group relationships; these are summarized in Table 3. For example, with respect to the core pseudomonad *phz* operon (Fig. 1), five (*phzADEF*G) of *B. cepacia*'s six *phz* genes share a sister-group relationship with pseudomonad core *phz* genes. Similarly five *S. cinnamonensis* (*phzACDE*G), *P. agglomerans* (*phzADEF*G),

and *P. atrosepticum* (*phzADEF*G) core *phz* genes are grouped among pseudomonad homologues (Table 3). These inferences agree with Blast-based database searches which show that these nonpseudomonad core *phz* genes have top hits to pseudomonad species and sequence similarity is also relatively high (Table 1). The most parsimonious solution for these observations is that a phenazine operon has independently transferred into these distantly related species. The supposition that *phz* genes were gained by some species through HGT is credible, as a ISXo8 transposase is found within 2 kb of the *M. abscessus* phenazine cluster (not shown). Furthermore, a DNA insertion element (transposase Bcep18194_B1576) is located beside the *B. cepacia* *phz* operon and several transposes lie in the vicinity of the *B. linens* core *phz* genes (not shown). The presence of transposases in these species is significant, because if their *phz* operon came from another bacterial donor, the vectors may have facilitated this transfer event.

Determining the *phz* operon donor species is not a facile task, however. Examination of *phz* phylogenetic inferences shows that the *phz* operon has had a checkered history. As has already been mentioned, previous researchers assumed that nonpseudomonad species have gained the *phz* operon from a pseudomonad source (Giddens et al. 2002). This assertion assumes that the *phz* operon originated de novo in *Pseudomonas*, followed by gene transfer to divergent species. If this scenario is the correct one, we would expect to see all *phz* core genes clustered together in a phylogeny (this is true for the majority of *phz* genes), and assuming artifact-free trees (e.g., long-branch attraction), the core *phz* genes should form a sister-group relationship with pseudomonad or closely related proteobacterial paralogues/homologues. This is definitely not the case for *phzC*, *phzD*, and *phzE*, where the corresponding phylogenies infer that the core *phz* genes have originated from an actinobacterial donor (Figs. 3–5). However, it is striking that most *phz* core genes display similar orientations (Fig. 1) and phylogenetic histories. Therefore, if we assume that the *phz* operon has been transferred en masse from a pseudomonad

Table 3 List of core *phz* genes in six bacterial species

	<i>phzA/B</i>	<i>phzC</i>	<i>phzD</i>	<i>phzE</i>	<i>phzF</i>	<i>phzG</i>
<i>B. cepacia</i>	SG	NSG	SG	SG	SG	SG
<i>P. atrosepticum</i>	SG	NA	SG	SG	SG	SG
<i>M. abscessus</i>	SG	SG	SG	SG	NA	SG
<i>B. linens</i>	SG	NSG	SG	SG	NSG	NA
<i>P. agglomerans</i>	SG	NA	SG	SG	SG	SG
<i>S. cinnamonensis</i>	SG	SG	SG	SG	NA	SG

Note: SG indicates where a *phz* homologue shares a sister-group relationship with a core pseudomonad *phz* gene. NSG indicates a non-sister-group relationship. N/A indicates the absence of a homologue

to divergent bacterial species, scenarios such as subsequent transfers back into actinobacterial species can be invoked to explain this hypothesis. However, it is important to note that these explanations are applicable to all species containing a *phz* operon (Fig. 1). Therefore one cannot confidently determine the donor species.

Interestingly there is one *B. cepacia* gene that does not share a sister-group relationship with the remaining PhzC proteins. Phylogenetic and Blast-based analyses suggest that *B. cepacia* gained *phzC* from a xanthomonad source (Fig. 3, Table 1). The operon structure of *B. cepacia* is very similar to that of *Pseudomonas aeruginosa* (Fig. 1). The one exception is the chromosomal position of *phzC*. The *phzC* in *B. cepacia* has been acquired from a xanthomonad source. It would be interesting to know the original integration site of the xanthomonad *phzC* in the *B. cepacia* genome. If it were different from its current location (Fig. 1), this would suggest that natural selection is shuffling the gene arrangement of *B. cepacia* through recombination to bring the xanthomonad *phzC* into the phenazine operon.

Overall this study has shown that the *phz* operon found in a number of diverse bacterial genomes has a common ancestry and has most likely moved between species through interspecies/phylum gene transfer. These findings, while novel, are unsurprising, as it has been proposed that genes encoding nonessential catabolic processes are more likely to be transferred than essential housekeeping genes (Jain et al. 1999). The acquisition of an operon associated with antibiotic properties could obviously increase the fitness of the recipient organism.

Acknowledgments I wish to thank two anonymous referees whose comments significantly improved the manuscript. I wish to acknowledge the financial support of the Irish Health Research Board (HRB). I also wish to acknowledge the SFI/HEA Irish Centre for High-End Computing (ICHEC) for the provision of computational facilities and support.

References

- Altschul SF, Madden TL, Schaffer AA, Zhang J, Zhang Z, Miller W, Lipman DJ (1997) Gapped BLAST and PSI-BLAST: a new generation of protein database search programs. *Nucleic Acids Res* 25:3389–3402 (Online)
- Bell KS, Sebahia M, Pritchard L, Holden MT, Hyman LJ, Holeva MC, Thomson NR, Bentley SD, Churcher LJ, Mungall K, Atkin R, Bason N, Brooks K, Chillingworth T, Clark K, Doggett J, Fraser A, Hance Z, Hauser H, Jagels K, Moule S, Norbertczak H, Ormond D, Price C, Quail MA, Sanders M, Walker D, Whitehead S, Salmond GP, Birch PR, Parkhill J, Toth IK (2004) Genome sequence of the enterobacterial phytopathogen *Erwinia carotovora* subsp. *atroseptica* and characterization of virulence factors. *Proc Natl Acad Sci USA* 101:11105–11110
- Bentley SD, Chater KF, Cerdeno-Tarraga AM, Challis GL, Thomson NR, James KD, Harris DE, Quail MA, Kieser H, Harper D, Bateman A, Brown S, Chandra G, Chen CW, Collins M, Cronin A, Fraser A, Goble A, Hidalgo J, Hornsby T, Howarth S, Huang CH, Kieser T, Larke L, Murphy L, Oliver K, O’Neil S, Rabinowitsch E, Rajandream MA, Rutherford K, Rutter S, Seeger K, Saunders D, Sharp S, Squares R, Squares S, Taylor K, Warren T, Wietzorrek A, Woodward J, Barrell BG, Parkhill J, Hopwood DA (2002) Complete genome sequence of the model actinomycete *Streptomyces coelicolor* A3(2). *Nature* 417:141–147
- Blankenfeldt W, Kuzin AP, Skarina T, Korniyenko Y, Tong L, Bayer P, Janning P, Thomashow LS, Mavrodi DV (2004) Structure and function of the phenazine biosynthetic protein PhzF from *Pseudomonas fluorescens*. *Proc Natl Acad Sci USA* 101:16431–16436
- Doolittle WF (1999) Phylogenetic classification and the universal tree. *Science* 284:2124–2129
- Edgar RC (2004) MUSCLE: multiple sequence alignment with high accuracy and high throughput. *Nucleic Acids Res* 32:1792–1797
- Eisen JA (2000) Assessing evolutionary relationships among microbes from whole-genome analysis. *Curr Opin Microbiol* 3:475–480
- Giddens SR, Feng Y, Mahanty HK (2002) Characterization of a novel phenazine antibiotic gene cluster in *Erwinia herbicola* Eh1087. *Mol Microbiol* 45:769–783
- Guindon S, Gascuel O (2003) A simple, fast, and accurate algorithm to estimate large phylogenies by maximum likelihood. *Syst Biol* 52:696–704
- Haagen Y, Gluck K, Fay K, Kammerer B, Gust B, Heide L (2006) A gene cluster for prenylated naphthoquinone and prenylated phenazine biosynthesis in *Streptomyces cinnamonensis* DSM 1042. *Chembiochem* 7:2016–2027
- Hassett DJ, Woodruff WA, Wozniak DJ, Vasil ML, Cohen MS, Ohman DE (1993) Cloning and characterization of the *Pseudomonas aeruginosa* *sodA* and *sodB* genes encoding manganese- and iron-cofactored superoxide dismutase: demonstration of increased manganese superoxide dismutase activity in alginate-producing bacteria. *J Bacteriol* 175:7658–7665
- Ikeda H, Ishikawa J, Hanamoto A, Shinose M, Kikuchi H, Shiba T, Sakaki Y, Hattori M, Omura S (2003) Complete genome sequence and comparative analysis of the industrial microorganism *Streptomyces avermitilis*. *Nat Biotechnol* 21:526–531
- Imamura N, Nishijima M, Takadera T, Adachi K, Sakai M, Sano H (1997) New anticancer antibiotics pelagiomicins, produced by a new marine bacterium *Pelagibacter variabilis*. *J Antibiot (Tokyo)* 50:8–12
- Jain R, Rivera MC, Lake JA (1999) Horizontal gene transfer among genomes: the complexity hypothesis. *Proc Natl Acad Sci USA* 96:3801–3806
- Jain R, Rivera MC, Moore JE, Lake JA (2003) Horizontal gene transfer accelerates genome innovation and evolution. *Mol Biol Evol* 20:1598–1602
- Keane TM, Creevey CJ, Pentony MM, Naughton TJ, McLnerney JO (2006) Assessment of methods for amino acid matrix selection and their use on empirical data shows that ad hoc assumptions for choice of matrix are not justified. *BMC Evol Biol* 6:29
- Kurland CG, Canback B, Berg OG (2003) Horizontal gene transfer: a critical view. *Proc Natl Acad Sci USA* 100:9658–9662
- Lartillot N, Philippe H (2004) A Bayesian mixture model for across-site heterogeneities in the amino-acid replacement process. *Mol Biol Evol* 21:1095–1099
- Lartillot N, Brinkmann H, Philippe H (2007) Suppression of long-branch attraction artefacts in the animal phylogeny using a site-heterogeneous model. *BMC Evol Biol* 7(Suppl 1):S4
- Lawrence JG, Ochman H (1997) Amelioration of bacterial genomes: rates of change and exchange. *J Mol Evol* 44:383–397

- Lockhart P, Steel M, Hendy M, Penny D (1994) Recovering evolutionary trees under a more realistic model of sequence. *Mol Biol Evol* 11:605–612
- Martin K, Morlin G, Smith A, Nordyke A, Eisenstark A, Golomb M (1998) The tryptophanase gene cluster of *Haemophilus influenzae* type b: evidence for horizontal gene transfer. *J Bacteriol* 180:107–118
- Mavrodi DV, Ksenzenko VN, Bonsall RF, Cook RJ, Boronin AM, Thomashow LS (1998) A seven-gene locus for synthesis of phenazine-1-carboxylic acid by *Pseudomonas fluorescens* 2–79. *J Bacteriol* 180:2541–2548
- Mavrodi DV, Bonsall RF, Delaney SM, Soule MJ, Phillips G, Thomashow LS (2001) Functional analysis of genes for biosynthesis of pyocyanin and phenazine-1-carboxamide from *Pseudomonas aeruginosa* PAOI. *J Bacteriol* 183:6454–6465
- Mavrodi DV, Blankenfeldt W, Thomashow LS (2006) Phenazine compounds in fluorescent *Pseudomonas* spp. biosynthesis and regulation. *Annu Rev Phytopathol* 44:417–445
- McDonald M, Mavrodi DV, Thomashow LS, Floss HG (2001) Phenazine biosynthesis in *Pseudomonas fluorescens*: branchpoint from the primary shikimate biosynthetic pathway and role of phenazine-1,6-dicarboxylic acid. *J Am Chem Soc* 123:9459–9460
- McInerney JO (1998) GCUA: general codon usage analysis. *Bioinformatics* 14:372–373
- Medigue C, Rouxel T, Vigier P, Henaut A, Danchin A (1991) Evidence for horizontal gene transfer in *Escherichia coli* speciation. *J Mol Biol* 222:851–856
- Ochman H, Lawrence JG, Groisman EA (2000) Lateral gene transfer and the nature of bacterial innovation. *Nature* 405:299–304
- Ohnishi Y, Ishikawa J, Hara H, Suzuki H, Ikenoya M, Ikeda H, Yamashita A, Hattori M, Horinouchi S (2008) Genome sequence of the streptomycin-producing microorganism *Streptomyces griseus* IFO 13350. *J Bacteriol* 190:4050–4060
- Parsons JF, Calabrese K, Eisenstein E, Ladner JE (2003) Structure and mechanism of *Pseudomonas aeruginosa* PhzD, an isochorismatase from the phenazine biosynthetic pathway. *Biochemistry* 42:5684–5693
- Parsons JF, Calabrese K, Eisenstein E, Ladner JE (2004a) Structure of the phenazine biosynthesis enzyme PhzG. *Acta Crystallogr D Biol Crystallogr* 60:2110–2113
- Parsons JF, Song F, Parsons L, Calabrese K, Eisenstein E, Ladner JE (2004b) Structure and function of the phenazine biosynthesis protein PhzF from *Pseudomonas fluorescens* 2–79. *Biochemistry* 43:12427–12435
- Rosas-Magallanes V, Deschavanne P, Quintana-Murci L, Brosch R, Gicquel B, Neyrolles O (2006) Horizontal transfer of a virulence operon to the ancestor of *Mycobacterium tuberculosis*. *Mol Biol Evol* 23:1129–1135
- Sato A, Takahashi S, Ogita T, Sugano M, Kodama K (1995) Marine natural products. *Annu Rep Sankyo Res Lab* 47:1–58
- Shimodaira H (2002) An approximately unbiased test of phylogenetic tree selection. *Syst Biol* 51:492–508
- Sidow A, Nguyen T, Speed TP (1992) Estimating the fraction of invariable codons with a capture-recapture method. *J Mol Evol* 35:253–260
- Snedecor GW, Cochran WG (1995) *Statistical methods*, 8th edn. Iowa State University Press, Ames
- Thollessen M (2004) LDDist: a Perl module for calculating LogDet pair-wise distances for protein and nucleotide sequences. *Bioinformatics (Oxford, England)* 20:416–418
- Turner JM, Messenger AJ (1986) Occurrence, biochemistry and physiology of phenazine pigment production. *Adv Microb Physiol* 27:211–275
- Woo PC, To AP, Lau SK, Yuen KY (2003) Facilitation of horizontal transfer of antimicrobial resistance by transformation of antibiotic-induced cell-wall-deficient bacteria. *Med Hypotheses* 61:503–508